

## High Efficient of Ca/Al-Graphite for Removal of Direct Orange

Yusuf Mathiinul Hakim<sup>1,3\*</sup>, Rananda Vinsiah<sup>2</sup>, Shahibul Fajri<sup>3</sup>

<sup>1</sup>Graduate School, Faculty of Mathematics and Natural Sciences, Sriwijaya University, Palembang, South Sumatera, 30139, Indonesia

<sup>2</sup>Department of Chemistry, Faculty of Mathematics and Natural Science, Sriwijaya University, Palembang, South Sumatera, 30139, Indonesia

<sup>3</sup>Research Center of Inorganic Materials and Coordination Complexes, Faculty of Mathematics and Natural Sciences, Sriwijaya University, Palembang, South Sumatera, 30139, Indonesia

\*Corresponding author: yusufmathiinul191@gmail.com

### Abstract

The layered double hydroxide-based material features of Ca/Al have improved according to the adsorption capacity and structure stabilization by transforming into composite Ca/Al-graphite. The composite was synthesized by co-precipitation method, and the chemical structure was characterized using X-ray Diffraction (XRD), Fourier Transform Infra-red (FT-IR), Brunauer-Emmet-Teller (BET) Surface Area, and Thermo-Gravimetry Differential Analyse (TG-DTA). The XRD analysis of Ca/Al-Graphite composite was noticed in 10.205°(003), 18.083°(012), 20.45°(004), 26.532°(002), 44.52°(101), 54.52°(004), and 77.38°(006). The TG-DTA analysis of the composite was noticed at 100°C as water molecule decomposition, 270°C as nitrate decomposition, and 700 and 760°C as graphite decomposition to the oxide form. BET surface area analysis of Ca/Al-Graphite composite achieved the highest surface area at 16.795 m<sup>2</sup>/g. According to the kinetic parameter, the adsorption of direct orange to composite follows the pseudo-second-order model. The isotherm parameter of direct orange adsorption onto the composite followed the Langmuir model and occurred spontaneously and endothermically. The regeneration study proved the composite effective in 3 cycles by adsorption percentage at the third cycle reached 73.559%.

### Keywords

Ca/Al Layered Double Hydroxide, Graphite, Composite, Adsorption, Direct Orange

Received: 3 January 2023, Accepted: 13 March 2023

<https://doi.org/10.26554/ijmr.2023112>

## 1. INTRODUCTION

Nowadays, industry activity has a rapid development. The industries included in the mass-production process are mining, textile, food and beverages, and pharmacy (Coimbra et al., 2019; Dutta et al., 2021; Hussain et al., 2020; Qasem et al., 2021). The textile industry impacted economic development and decreased environmental quality due to the high volume of dye waste released (Czatkowska et al., 2022). Dye waste containing different reactive and dissolved dye structures, can spread widely causing the carcinogenic-mutagenic effect on living organisms. Direct orange is a representative dye commonly used in the textile until the food industry has toxic characteristics due to azo structure (Krewski et al., 2019).

Different wastewater treatment methods were studied, and adsorption was chosen as simple, effective, and economically better than conventional removal methods (Rashid et al., 2021). As an essential part of adsorption, the adsorbent was modified to be effective in the reusable mechanism. Adsorbent was utilized due to the active site to catch the pollutant of wastewater and the unique characteristics of adsorbent, including the high surface area, small size, and ion exchange from layered

material (Lim et al., 2019). Popular adsorbent include charcoal, biochar, zeolite, and layered double hydroxide (LDH). LDH is a group of two-dimensional layered inorganic materials. LDH has unique characteristics of adjustable composition, high surface area, structural memory effect, and reusability (Siregar et al., 2022).

The adjustable composition of LDH becomes a shining issue since it can be compiled as an  $M_{1-x}^{2+}M_x^{3+}$  structure, where the  $M^{2+}$  and  $M^{3+}$  are divalent metal cations (Ca, Mg, Co, Fe, Cu, Ni, Mn) and trivalent metal cation (Al, Fe, Cr), respectively (Hanifah et al., 2023). The two-dimensional divalent-trivalent metal cation piled up in several layered and provided a basal space that exchangeable anion can fill up. In aims to provide a high-efficient adsorbent, the LDH modification mechanism based on memory effects such are self-assembly, ion exchange, and delamination. It is considered an effective method to achieve a multifunctional material based on LDH using host materials (Ye et al., 2022). The host materials generally used in LDH modification include semiconductors, carbon, metal, and other LDH materials (Hong et al., 2014; Malak-Polaczyk et al., 2010; Yang et al., 2019).

Graphite is classified as carbon-based material, usually used

in the composite matrix. Recently, graphite has also been considered an efficient adsorbent. Normah et al. (2021b) recently modified the LDH of Ni-Al composited to graphite and achieved stability structure of LDH materials with adsorption capacity at 72.464 mg/g. The graphite structure of the carbon web provides growth space for LDH particles upon the graphite surfaces. This combination significantly improves the adsorption ability. In addition, Hu et al. (2020) summarized the information about the agglomeration-avoid feature from carbon-based material, which is composited to LDH material. It triggers an increase of specific surface area in the adsorbent.

According to Hu et al. (2020), the composite of Ni/Fe-LDH to carbon-based material significantly drives the maximum capacity to 323.6 and 448.4 mg/g to methyl orange and congo red dyes, respectively. Dinari et al. (2020) have reported the successful preparation of Ni/Co-LDH composited to carbon nanotube material and increased the surface area from 5.19 to 52.63 m<sup>2</sup>/g. Additionally, the composite material has stabilized the LDH structure and increased the reusability. This statement was proven by Suh et al. (2020), which examined the Mg/Al-LDH composited with TiO<sub>2</sub> and achieved 97% removal of methyl orange for five cycles.

This work reported the successfully formed Ca/Al-graphite composite using the co-precipitation method. The effectiveness of material ability in dye waste removal was examined directly to remove the direct orange (DO) contaminant. The final material was characterized using XRD, FT-IR, BET, and TGA analysis. The regeneration adsorption of this material was also observed in three cycles in different wash solutions to know the effectiveness of the composite in DO removal.

## 2. EXPERIMENTAL SECTION

### 2.1 Chemicals and Instrumentation

All chemicals in pure grade condition, including calcium nitrate tetrahydrate (Ca(NO<sub>3</sub>)<sub>2</sub>·4H<sub>2</sub>O) purchased from Sigma Aldrich, aluminum nitrate nonahydrate (Al(NO<sub>3</sub>)<sub>3</sub>·9H<sub>2</sub>O) purchased from Sigma Aldrich, graphite powder purchased from Merck, sodium hydroxide (NaOH) purchased from Merck, chloride acid (HCl) purchased from Ajax Finechem, ethanol purchased from Avantor, and distilled water. Instrumentations were used in this work, including X-Ray Diffraction (XRD) type Rigaku MiniFlex 600 in a scan range 2θ 5-80°, Fourier Transform Infra-Red (FT-IR) type NOVA 4200e in a scan range wavenumber 400-3800 cm<sup>-1</sup>, ASAP 2020 Surface Area Analyzer based on BET calculation, and TGA analyzer type Shimadzu DTG-60H with range analysis temperature of 27-900°C. Dye concentration reduction was analyzed by Bio-base BK-UV 1800 PC Spectrophotometer UV-Vis at 497 nm.

### 2.2 Synthesis of Ca/Al (LDH)

Ca/Al (LDH) was synthesized by homogenizing 100 mL Ca(NO<sub>3</sub>)<sub>2</sub>·4H<sub>2</sub>O 0.75 M and 100 mL Al(NO<sub>3</sub>)<sub>3</sub>·9H<sub>2</sub>O 0.25 M in 30 minutes of stirring. Then the pH solution was controlled at 10 using NaOH 2M. The solution was stirred at 65°C for 24 hours. Then, the precipitate was filtered and washed using distilled water to

reduce the impurities. Finally, the precipitate was oven-dried at 100°C overnight.

### 2.3 Synthesis of Ca/Al-Graphite

Ca/Al-Graphite composite was synthesized using the co-precipitation method under alkaline conditions (pH 10). A solution of 15 mL Ca(NO<sub>3</sub>)<sub>2</sub>·4H<sub>2</sub>O 0.75 M and 15 mL Al(NO<sub>3</sub>)<sub>3</sub>·9H<sub>2</sub>O 0.25 M were homogenized, and then 3 g of graphite was added. The pH solution was kept at 10 using NaOH 2 M and stirred at 65°C for 24 hours. The precipitate was filtered and washed using distilled water. Then it was oven-dried at 100°C overnight.

### 2.4 Adsorption Study

The adsorption study was carried out with pH, contact time, initial concentration, and temperature parameters. The effect of pH was carried out by controlling the pH of 25 mL DO 50 mg/L solution in a range of 2-11 using HCl 0.1 M and NaOH 0.1 M, followed by an adsorption process using 0.05 g adsorbent for 120 minutes stirring. The effect of contact time was examined by preparing 0.05 g adsorbent in 25 mL direct orange 50 mg/L solution and varying adsorption time in 0-200 minutes. The effect of initial concentration and temperatures was carried out by varying the dye concentration to 50, 75, 100, 125, and 150 mg/L and varying the temperatures in a range of 30-60°C. Then the adsorption reached in a system of 0.05 g adsorbent in 20 mL DO solution.

### 2.5 Regeneration Study

An adsorption-desorption mechanism examined the regeneration. The adsorption process using 20 mL DO 100 mg/L, repeatedly. Then, the desorption process using 20 mL of different solutions (distilled water, NaOH 1 M, HCl 1 M, acetone 1 M, and ethanol 1 M solution) under 120 minutes of stirring. The concentration excess of dye solution for every cycle was measured using a spectrophotometer UV-Vis.

## 3. RESULTS AND DISCUSSION

Ca/Al-graphite composite as functionalized material was characterized using XRD, FT-IR, BET, and TGA to observe the crystal structure changes, structure bonding that formed, surface area improvement, and structure transformation according to the different temperatures (Botan and de Bona Sartor, 2020; Cardinale et al., 2022; Shabaniyan et al., 2020; Walton and Snurr, 2007). Figure 1 shows the XRD pattern of the Ca/Al-graphite composite, which figures out the unique peak in every precursor of LDH and graphite. The peak of Ca/Al (LDH) is shown in 2θ of 10.205°(003), 18.083°(012), and 20.45°(004), while the composited graphite's peak is shown in 2θ of 26.532°(002), 44.52°(101), 54.52°(004), and 77.38°(006) (Siregar et al., 2022; Vinsiah et al., 2020; Wei et al., 2020). The peak at 10.205° is the basal spacing of Ca/Al (LDH). The low peak intensity of graphite was noticed as an amorphous structure (Vinsiah et al., 2020).

Figure 2 figured out the FT-IR analyses of the Ca/Al-graphite composite and shows several specific peaks owned by the LDH and graphite structure that united. The wide band detected

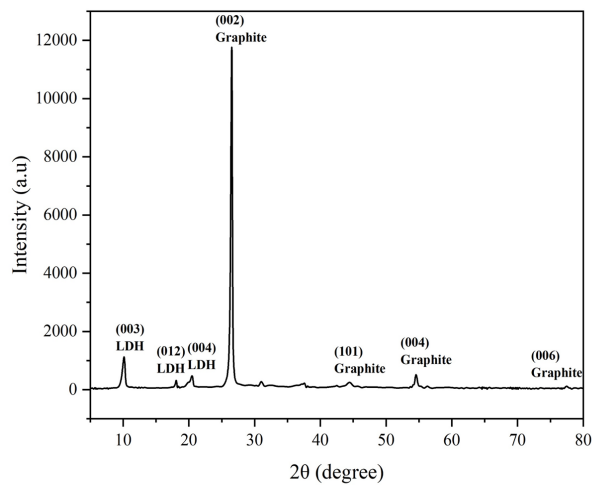


**Figure 1.** XRD Pattern of Ca/Al-Graphite Composite

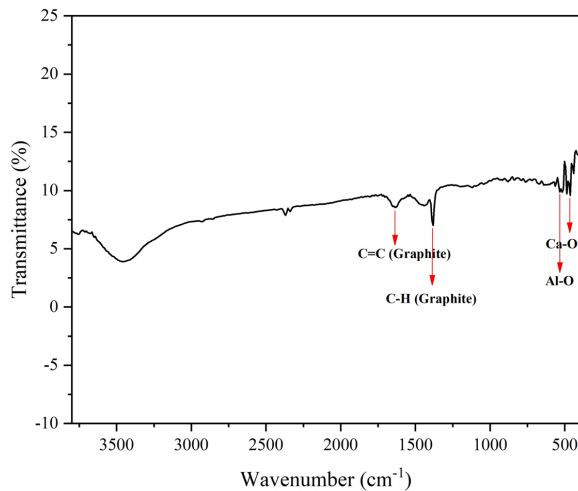


**Figure 2.** FT-IR Spectrum Analysis of Ca/Al-Graphite Composite

at  $3456\text{ cm}^{-1}$  as O-H vibration from water molecules located between the interlayer of LDH (Shabanian et al., 2020). Then, the duplet band located at  $516$  and  $640\text{ cm}^{-1}$  was detected as metal-oxygen binding from the LDH structure (Ca-O and Al-O, respectively) (Siregar et al., 2022). Moreover, the double band at  $1635$  and  $1381\text{ cm}^{-1}$  was detected as C=C and C-H binding from graphite web structure (Vinsiah et al., 2020).

The thermal behavior of the Ca/Al-graphite composite was carried out using a TGA instrument with nitrogen media, and the result was figured out in Figure 3. The dehydration process as water molecules decomposition from the composite structure was detected at  $100^\circ\text{C}$  (Kanungo and Mishra, 1996). Nitrate molecules loss by thermal decomposition was detected at  $270^\circ\text{C}$  (Zhao et al., 2022). Furthermore, double decreasing area at  $700$

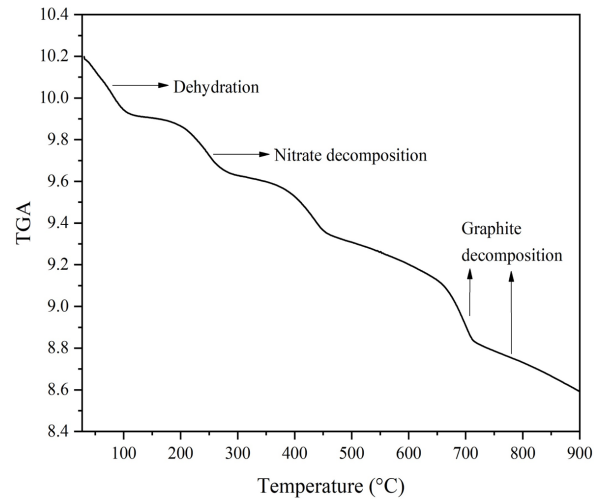


**Figure 3.** TGA Pattern on Ca/Al-Graphite Composite Analysis

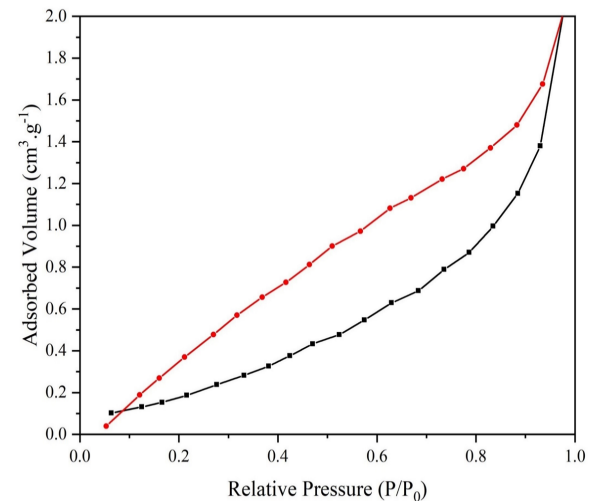


**Figure 4.** BET Model Profile of Ca/Al-Graphite Composite

and  $760^\circ\text{C}$  detected as graphite structure decomposition and transforming to oxide form (Zhang et al., 2018).

The surface area analysis was carried out using the BET model isotherm, and the result is shown in Figure 4. The adsorption-desorption plot shape fitted to type IV, which is indicated by the formation of a hysteresis loop (Mohadi et al., 2023). In detail, this explains that the gas capillary condensation occurred in the mesopore at relatively high pressure. The loop hysteresis shows a narrow edge and wide body classified as H2-type (Cychosz and Thommes, 2018). The analysis calculated the surface area as  $16.795\text{ m}^2/\text{g}$  with pore volume and diameter of  $0.040\text{ cm}^3/\text{g}$  and  $2.897\text{ nm}$ , respectively. The composite mechanism has repaired the particle size and pore condition (Monakhova et al., 2021).

The adsorption study was initiated by screening the optimum pH in the adsorption system at 2-11. The optimum pH adsorption

**Table 1.** Kinetic Parameter for DO Adsorption

Dye	Initial Concentration (mg/L)	Q <sub>experiment</sub> (mg/g)	PFO		PSO			
			Q <sub>e-calc</sub> (mg/g)	R <sup>2</sup>	K <sub>1</sub>	Q <sub>e-calc</sub> (mg/g)	R <sup>2</sup>	K <sub>2</sub>
DO	50	48.023	284.577	0.878	0.033	55.248	0.971	0.0007

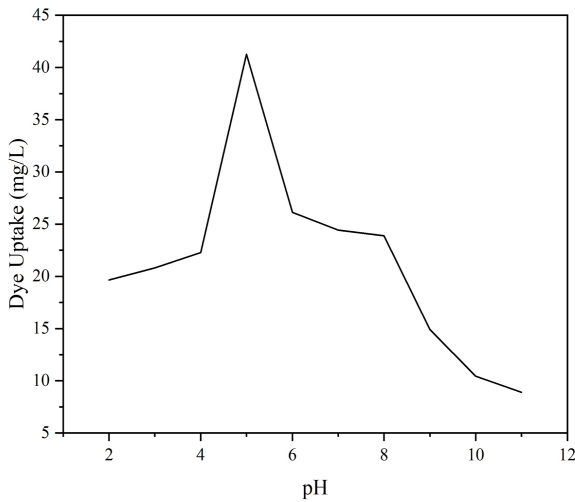


**Figure 5.** Plotting of pH Optimum Adsorption of DO onto Ca/Al-Graphite Composite

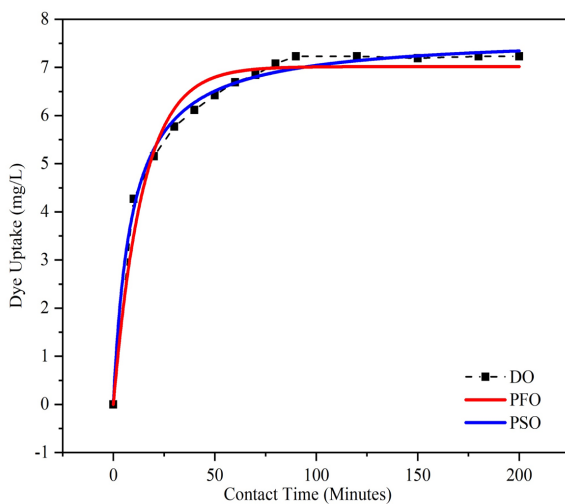


**Figure 6.** The Effect of Contact Time Adsorption of DO on Ca/Al-Graphite and the Fitting Toward Kinetic Model Adsorption

of DO using Ca/Al-graphite composite was achieved at 5, and the result was plotted in Figure 5. The acid condition from the optimum pH triggers protonation at composite surfaces and promotes the adsorption process by providing a binding site for

**Table 2.** Isotherm Parameters for DO Adsorption

Temperature (°C)	Model of Isotherm Adsorption					
	Langmuir			Freundlich		
	Q <sub>max</sub>	KL	R <sup>2</sup>	n	KF	R <sup>2</sup>
30	10.010	0.089	0.980	0.425	1.731	0.928
40	105.263	0.114	0.988	0.498	5.176	0.898
50	111.111	0.139	0.993	0.532	2.251	0.904
60	112.36	0.214	0.998	0.909	1.527	0.996

the DO dye as an anionic dye (Normah et al., 2021a). The pH 5 gives appropriate composition in providing an active site and functional group that optimizes the adsorption system of the adsorbent. A considerable amount of dye particles adsorbed in this pH range suggests involvement in chemical interaction, such as hydrogen bonding, Van der Waals force, and hydrophobic interaction (Mahmoud et al., 2021). Furthermore, the increasing pH value triggers decreasing adsorption capacity due to the competitive effect between -OH from the solution's alkaline condition and the dyes' anion charge (Yadav and Dasgupta, 2022).

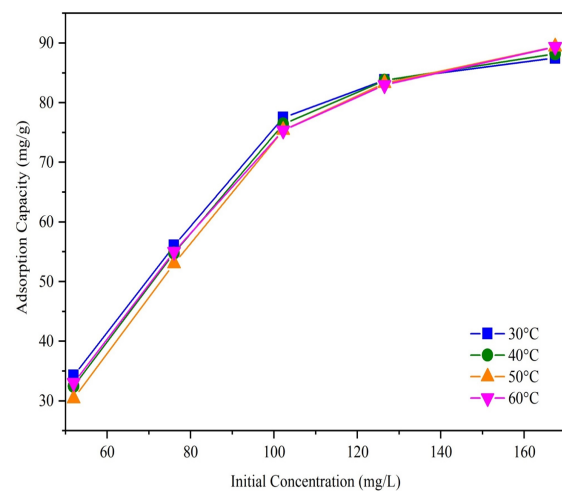


**Figure 7.** The Effect of Temperature and Concentration of DO Adsorption on Ca/Al-Graphite Composite

The effect of contact time in DO adsorption onto Ca/Al-graphite composite was calculated using the kinetic adsorption model of the pseudo-first-order (PFO) and pseudo-second-order (PSO) equations. The analysis result is shown in Figure 6 (Mo-

**Table 3.** Thermodynamic Parameters for DO Adsorption

Concentration (mg/L)	T (°C)	Qe (mg/g)	$\Delta H$ (kJ/mol)	$\Delta S$ (kJ/mol.K)	$\Delta G$ (kJ/mol)
50	30	34.231	27.528	0.096	-1.578
	40	37.462			-2.538
	50	40.385			-3.499
	60	43.615			-4.459
75	30	56.023	27.256	0.098	-2.483
	40	59.792			-3.464
	50	63.023			-4.446
	60	67.177			-5.425
100	30	77.485	21.306	0.080	-2.822
	40	81.408			-3.619
	50	85.408			-4.415
	60	88.946			-5.211
125	30	83.792	14.595	0.054	-1.692
	40	88.715			-2.230
	50	93.254			-2.767
	60	97.1			-3.305
150	30	87.531	11.410	0.038	-0.226
	40	93.223			-0.610
	50	99.377			-0.994
	60	103.992			-1.378

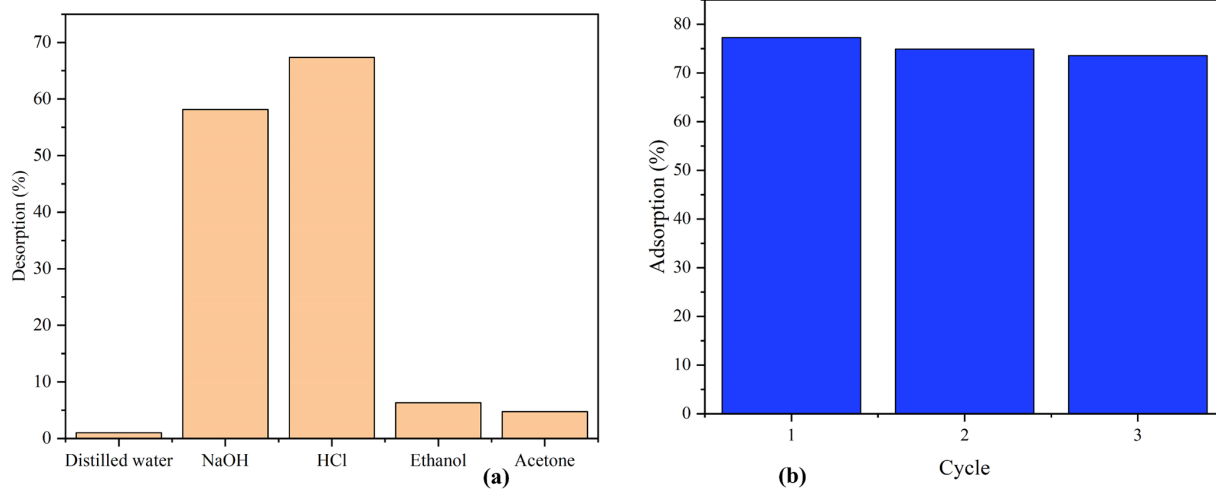


**Figure 8.** Effectiveness of Different Solutions on DO Desorption (a) and Degree of Regeneration Adsorbent (b)

hadi et al., 2018). According to the fit-test, the trend of kinetic adsorption follows the PSO of the kinetic adsorption model. According to Hakim et al. (2023), the PSO model explains that the interaction in the adsorption of the adsorbate occurs through the chemisorption mechanism. The kinetic parameter is shown in Table 1.

The effect of different temperatures and initial concentration adsorption was observed using the isotherm and thermodynamic adsorption model. The isotherm adsorption analysis was calculated by Langmuir and Freundlich's model equation (Freundlich, 1907; Langmuir, 1916). According to Chung et al. (2015), the differences between Langmuir and Freundlich models are assuming the adsorption scheme occurs by monolayer (directly adsorbate to adsorbent) and multilayer (growth in heterogeneous places), respectively. According to Figure 7, the result of isotherm adsorption analysis follows the Langmuir adsorption model, meaning the adsorption occurs in a monolayer (chemisorption) (Taher et al., 2018; Taher et al., 2019). This statement was supported by Table 2 data showing the higher  $R^2$  value in the Langmuir adsorption model. The maximum adsorption capacity of Ca/Al-graphite composite toward DO dye is 112.36 mg/g.

The thermodynamic adsorption analysis was achieved by calculating the enthalpy ( $\Delta H$ ), entropy ( $\Delta S$ ), and Gibbs free energy ( $\Delta G$ ) equation (Motomura, 1978). According to Table 3, the thermodynamic parameters show several essential points, including the positive value of  $\Delta H$  that indicates the adsorption optimal occurs by endothermic, the positive value of  $\Delta S$  that indicates the DO adsorption reaction feasible in the increasing degree of freedom, and the negative value of  $\Delta G$  that means the adsorption occurs spontaneously (Hakim et al., 2023; Siregar et al., 2022; Sahmoune, 2019). The adsorption capacity tends to increase aligned with increasing temperature because the high temperature can overcome the repulsive forces in the adsorption system. This statement supports by the  $\Delta G$  value (Malima et al., 2021).

The regeneration study includes the adsorption and desorption schemes. The desorption scheme was initiated by screening the washer solution. According to Figure 8a, the HCl solution provides the highest desorption ability, meaning it has the highest ability to cut the DO binding to the adsorbent (Moyo, 2013; Pan et al., 2022). Furthermore, in Figure 8b, Ca/Al-graphite composite regeneration shows considerable ability due to the high adsorption percentage after three cycles, with 73.559% removal at the third cycle.

#### 4. CONCLUSIONS

The collaborative material of the Ca/Al-graphite composite was successfully formed using the co-precipitation method. The XRD analysis confirmed the compositing result by figuring out the Ca/Al (LDH) and graphite peaks in an XRD graph. Adsorption features of surface area from the Ca/Al-graphite composite were achieved at 16.795  $m^2/g$ . According to the adsorption study, the optimum removal of the DO occurred at a pH of 5 for 120 minutes of adsorption. The adsorption capacity of the Ca/Al-graphite composite is 112.360 mg/g. The Ca/Al-graphite composite's

regeneration work showed proper desorption using an HCl solution and achieved a stable DO removal for three cycles with 73.559% removal at the third cycle.

#### 5. ACKNOWLEDGEMENT

All authors thank the Research Center of Inorganic Materials and Coordination Complexes, Faculty of Mathematics and Natural Sciences, Sriwijaya University, for supporting this research.

#### REFERENCES

- Botan, R. and S. de Bona Sartor (2020). X-Ray Diffraction Analysis of Layered Double Hydroxide Polymer Nanocomposites. In *Layered Double Hydroxide Polymer Nanocomposites*. Elsevier; 205–229
- Cardinale, A. M., M. Fortunato, F. Locardi, and N. Parodi (2022). Thermal Analysis of MgFe-Cl Layered Doubled Hydroxide (LDH) Directly Synthesized and Produced "Via Memory Effect". *Journal of Thermal Analysis and Calorimetry*, **147**(9); 5297–5302
- Chung, H.-K., W.-H. Kim, J. Park, J. Cho, T.-Y. Jeong, and P.-K. Park (2015). Application of Langmuir and Freundlich isotherms to Predict Adsorbate Removal Efficiency or Required Amount of Adsorbent. *Journal of Industrial and Engineering Chemistry*, **28**; 241–246
- Coimbra, R., V. Calisto, C. Ferreira, V. Esteves, and M. Otero (2019). Removal of Pharmaceuticals from Municipal Wastewater by Adsorption Onto Pyrolyzed Pulp Mill Sludge. *Arabian Journal of Chemistry*, **12**(8); 3611–3620
- Cychosz, K. A. and M. Thommes (2018). Progress in the Physisorption Characterization of Nanoporous Gas Storage Materials. *Engineering*, **4**(4); 559–566
- Czatkowska, M., I. Wolak, M. Harnisz, and E. Korzeniewska (2022). Impact of Anthropogenic Activities on the Dissemination of ARGs in the Environment—A Review. *International Journal of Environmental Research and Public Health*, **19**(19); 12853
- Dinari, M., H. Allami, and M. M. Momeni (2020). A High-Performance Electrode Based on Ce-Doped Nickel-Cobalt Layered Double Hydroxide Growth on Carbon Nanotubes for Efficient Oxygen Evolution. *Journal of Electroanalytical Chemistry*, **877**; 114643
- Dutta, S., B. Gupta, S. K. Srivastava, and A. K. Gupta (2021). Recent Advances on the Removal of Dyes from Wastewater using Various Adsorbents: A Critical Review. *Materials Advances*, **2**(14); 4497–4531
- Freundlich, H. (1907). Über Die Adsorption in Lösungen. *Zeitschrift Für Physikalische Chemie*, **57**(1); 385–470
- Hakim, Y. M., R. Mohadi, M. Mardiyanto, and I. Royani (2023). Ammonium-Assisted Intercalation of Java Bentonite as Effective of Cationic Dye Removal. *Journal of Ecological Engineering*, **24**(2); 184–195
- Hanifah, Y., R. Mohadi, M. Mardiyanto, and A. Lesbani (2023). Polyoxometalate Intercalated MgAl-Layered Double Hydrox-

- ide for Degradation of Malachite Green. *Ecological Engineering & Environmental Technology*, **24**(2); 109–119
- Hong, J., W. Zhang, Y. Wang, T. Zhou, and R. Xu (2014). Photocatalytic Reduction of Carbon Dioxide Over Self-Assembled Carbon Nitride and Layered Double Hydroxide: The Role of Carbon Dioxide Enrichment. *ChemCatChem*, **6**(8); 2315–2321
- Hu, H., S. Wageh, A. A. Al-Ghamdi, S. Yang, Z. Tian, B. Cheng, and W. Ho (2020). NiFe-LDH Nanosheet/Carbon Fiber Nanocomposite with Enhanced Anionic Dye Adsorption Performance. *Applied Surface Science*, **511**; 145570
- Hussain, S., N. Khan, S. Gul, S. Khan, and H. Khan (2020). Contamination of Water Resources by Food Dyes and its Removal Technologies. *Water Chemistry*; 1–14
- Kanungo, S. and S. Mishra (1996). Thermal Dehydration and Decomposition of  $\text{FeCl}_{3x}\text{H}_2\text{O}$ . *Journal of Thermal Analysis*, **46**; 1487–1500
- Krewski, D., M. Bird, M. Al-Zoughool, N. Birkett, M. Billard, B. Milton, J. M. Rice, Y. Grosse, V. J. Cogliano, and M. A. Hill (2019). Key Characteristics of 86 Agents Known to Cause Cancer in Humans. *Journal of Toxicology and Environmental Health, Part B*, **22**(7-8); 244–263
- Langmuir, I. (1916). The Constitution and Fundamental Properties of Solids and Liquids. Part I. Solids. *Journal of the American Chemical Society*, **38**(11); 2221–2295
- Lim, K., J. Kim, and J. Lee (2019). Comparative Study on Adsorbent Characteristics for Adsorption Thermal Energy Storage System. *International Journal of Energy Research*, **43**(9); 4281–4294
- Mahmoud, R. K., M. Taha, A. Zaher, and R. M. Amin (2021). Understanding the Physicochemical Properties of Zn–Fe LDH Nanostructure as Sorbent Material for Removing of Anionic and Cationic Dyes Mixture. *Scientific Reports*, **11**(1); 21365
- Malak-Polaczyk, A., C. Vix-Guterl, and E. Frackowiak (2010). Carbon/Layered Double Hydroxide (LDH) Composites for Supercapacitor Application. *Energy & Fuels*, **24**(6); 3346–3351
- Malima, N., S. Owonubi, E. Lugwisha, and A. Mwakaboko (2021). Thermodynamic, Isothermal and Kinetic Studies of Heavy Metals Adsorption by Chemically Modified Tanzanian Malangali Kaolin Clay. *International Journal of Environmental Science and Technology*, **18**(10); 1–16
- Mohadi, R., Y. M. Hakim, R. D. Astuti, I. Royani, and M. Mardiyanto (2023). Pillarization of Sumatera Bentonite by Sodium-assisted as Effective Adsorbent of Anionic Surfactants Sodium Lauryl Sulphate (SLS) Waste. *Bulletin of Chemical Reaction Engineering & Catalysis*, **18**(1); 48–58
- Mohadi, R., D. Setiawan, and H. Zulkifli (2018). Kinetic and Thermodynamic Adsorption of Cr(VI) onto Dried *Oscillatoria Splendida* in Aqueous Solution. *Science and Technology Indonesia*, **3**(4); 195–198
- Monakhova, K., S. Bazhenov, A. Keчек'yan, and I. Meshkov (2021). Effect of the Size of Particles on Their Adhesion in Composite Polypropylene/SiO<sub>2</sub>. *Polymer Science, Series A*, **63**; 162–171
- Motomura, K. (1978). Thermodynamic Studies on Adsorption at Interfaces. I. General Formulation. *Journal of Colloid and Interface Science*, **64**(2); 348–355
- Moyo, M. (2013). Bioremediation of Lead(II) from Polluted Wastewaters Employing Sulphuric Acid Treated Maize Tassel Biomass. *American Journal of Analytical Chemistry*, **4**(12); 689
- Normah, N., N. Juleanti, P. M. S. B. N. Siregar, A. Wijaya, N. R. Palapa, T. Taher, and A. Lesbani (2021a). Size Selectivity of Anionic and Cationic Dyes using LDH Modified Adsorbent with Low-Cost Rambutan Peel to Hydrochar. *Bulletin of Chemical Reaction Engineering & Catalysis*, **16**(4); 869–880
- Normah, N., N. R. Palapa, T. Taher, R. Mohadi, H. P. Utami, and A. Lesbani (2021b). The Ability of Composite Ni/Al-Carbon Based Material Toward Readsorption of Iron(II) in Aqueous Solution. *Science and Technology Indonesia*, **6**(3); 156–165
- Pan, Y., Y. Liu, Z. Tu, X. Zhang, Y. Wu, and X. Hu (2022). Highly Efficient Absorption of HCl in Deep Eutectic Solvents and Their Corresponding Ethylene Glycol Blends. *Chemical Engineering Journal*, **434**; 134707
- Qasem, N. A., R. H. Mohammed, and D. U. Lawal (2021). Removal of Heavy Metal Ions from Wastewater: a Comprehensive and Critical Review. *Npj Clean Water*, **4**(1); 36
- Rashid, R., I. Shafiq, P. Akhter, M. J. Iqbal, and M. Hussain (2021). A State-of-the-Art Review on Wastewater Treatment Techniques: the Effectiveness of Adsorption Method. *Environmental Science and Pollution Research*, **28**; 9050–9066
- Sahmoune, M. N. (2019). Evaluation of Thermodynamic Parameters for Adsorption of Heavy Metals by Green Adsorbents. *Environmental Chemistry Letters*, **17**(2); 697–704
- Shabanian, M., M. Hajibeygi, and A. Raeisi (2020). FTIR Characterization of Layered Double Hydroxides and Modified Layered Double Hydroxides. In *Layered Double Hydroxide Polymer Nanocomposites*. Elsevier; 77–101
- Siregar, P. M. S. B. N., A. Wijaya, J. P. Nduru, N. Hidayati, A. Lesbani, and R. Mohadi (2022). Layered Double Hydroxide/C (C=Humic Acid; Hydrochar) as Adsorbents of Cr (VI). *Science and Technology Indonesia*, **7**(1); 41–48
- Suh, M. J., S. Weon, R. Li, P. Wang, and J. H. Kim (2020). Enhanced Pollutant Adsorption and Regeneration of Layered Double Hydroxide-Based Photoregenerable Adsorbent. *Environmental Science & Technology*, **54**(14); 9106–9115
- Taher, T., D. Rohendi, R. Mohadi, and A. Lesbani (2018). Thermal and Acid Activation (TAA) of Bentonite as Adsorbent for Removal of Methylene Blue: a Kinetics and Thermodynamic Study. *Chiang Mai Journal of Science*, **45**(4); 1770–1781
- Taher, T., D. Rohendi, R. Mohadi, and A. Lesbani (2019). Congo Red Dye Removal from Aqueous Solution by Acid-Activated Bentonite from Sarolangun: Kinetic, Equilibrium, and Thermodynamic Studies. *Arab Journal of Basic and Applied Sciences*, **26**(1); 125–136
- Vinsiah, R., R. Mohadi, and A. Lesbani (2020). Performance of Graphite for Congo Red and Direct Orange Adsorption. *Indonesian Journal of Environmental Management and Sustainability*, **4**(4); 125–132
- Walton, K. S. and R. Q. Snurr (2007). Applicability of the BET Method for Determining Surface Areas of Microporous Metal-Organic Frameworks. *Journal of the American Chemical Society*

- ety, **129**(27); 8552–8556
- Wei, L., F. Zietzschmann, L. C. Rietveld, and D. van Halem (2020). Fluoride Removal by Ca-Al-CO<sub>3</sub> Layered Double Hydroxides at Environmentally-Relevant Concentrations. *Chemosphere*, **243**; 125307
- Yadav, B. S. and S. Dasgupta (2022). Effect of Time, pH, and Temperature on Kinetics for Adsorption of Methyl Orange Dye Into the Modified Nitrate Intercalated MgAl LDH Adsorbent. *Inorganic Chemistry Communications*; 109203
- Yang, R., Y. Zhou, Y. Xing, D. Li, D. Jiang, M. Chen, W. Shi, and S. Yuan (2019). Synergistic Coupling of CoFe-LDH Arrays with NiFe-LDH Nanosheet for Highly Efficient Overall Water Splitting in Alkaline Media. *Applied Catalysis B: Environmental*, **253**; 131–139
- Ye, H., S. Liu, D. Yu, X. Zhou, L. Qin, C. Lai, F. Qin, M. Zhang, W. Chen, and W. Chen (2022). Regeneration Mechanism, Modification Strategy, and Environment Application of Layered Double Hydroxides: Insights Based on Memory Effect. *Coordination Chemistry Reviews*, **450**; 214253
- Zhang, G., M. Wen, S. Wang, J. Chen, and J. Wang (2018). Insights Into Thermal Reduction of the Oxidized Graphite from the Electro-Oxidation Processing of Nuclear Graphite Matrix. *RSC Advances*, **8**(1); 567–579
- Zhao, A., B. Xiong, Y. Han, and H. Tong (2022). Thermal Decomposition Paths of Calcium Nitrate Tetrahydrate and Calcium Nitrite. *Thermochimica Acta*, **714**; 179264